


SHORT COMMUNICATION

Comprehensive immune cell profiling depicts an early immune response associated with severe coronavirus disease 2019 in cancer patients

Prashant R Tembhare¹ , Harshini Sriram¹, Gaurav Chatterjee¹, Twinkle Khanka¹, Anant Gokarn², Sumeet Mirgh², Akhil Rajendra², Anumeha Chaturvedi¹, Sitaram G Ghogale¹, Nilesh Deshpande¹, Karishma Girase¹, Kajal Dalvi¹, Sweta Rajpal¹, Nikhil Patkar¹, Bhakti Trivedi³, Amit Joshi², Vedang Murthy⁴, Nitin Shetty⁵, Sudhir Nair⁶, Ashwini More⁷, Sujeet Kamtalwar⁷, Preeti Chavan⁸, Vivek Bhat⁸, Prashant Bhat⁹, Papagudi G Subramanian¹, Sudeep Gupta² & Navin Khattry²

¹ Hematopathology Laboratory, ACTREC, Tata Memorial Center, Homi Bhabha National Institute (HBNI) University, Mumbai, India

² Department of Medical Oncology, ACTREC, Tata Memorial Center, HBNI University, Mumbai, India

³ Department of Anesthesiology, Critical Care and Pain, Tata Memorial Center, HBNI University, Mumbai, India

⁴ Department of Radiation Oncology, ACTREC, Tata Memorial Center, HBNI University, Mumbai, India

⁵ Department of Radio-Diagnosis, ACTREC, Tata Memorial Center, HBNI University, Mumbai, India

⁶ Department of Head and Neck Surgical Oncology, ACTREC, Tata Memorial Center, HBNI University, Mumbai, India

⁷ Department of Medicine, ACTREC, Tata Memorial Center, HBNI University, Mumbai, India

⁸ Composite Laboratory and Microbiology, ACTREC, Tata Memorial Center, HBNI University, Mumbai, India

⁹ Medical Administration, ACTREC, Tata Memorial Center, HBNI University, Mumbai, India

Keywords

Cancer patients, COVID-19, immune cell profile, inflammatory cytokines, myeloid dendritic cells, SARS-CoV-2, severe disease

Corresponding

Prashant R Tembhare, Hematopathology Laboratory, ACTREC, Tata Memorial Center, Homi Bhabha National Institute (HBNI) University, CCE Building, ACTREC, Mumbai 410210, Maharashtra, India.
Emails: docprt@gmail.com;
ptembhare@actrec.gov.in

Received 4 June 2021;

Revised 22 August,

25 and 26 September 2021;

Accepted 27 September 2021

doi: 10.1111/imcb.12504

Immunology & Cell Biology 2022; 100: 61–73

Abstract

Recent studies have highlighted multiple immune perturbations related to severe acute respiratory syndrome coronavirus 2 infection-associated respiratory disease [coronavirus disease 2019 (COVID-19)]. Some of them were associated with immunopathogenesis of severe COVID-19. However, reports on immunological indicators of severe COVID-19 in the early phase of infection in patients with comorbidities such as cancer are scarce. We prospectively studied about 200 immune response parameters, including a comprehensive immune-cell profile, inflammatory cytokines and other parameters, in 95 patients with COVID-19 (37 cancer patients without active disease and intensive chemo/immunotherapy, 58 patients without cancer) and 21 healthy donors. Of 95 patients, 41 had severe disease, and the remaining 54 were categorized as having a nonsevere disease. We evaluated the association of immune response parameters with severe COVID-19. By principal component analysis, three immune signatures defining characteristic immune responses in COVID-19 patients were found. Immune cell perturbations, in particular, decreased levels of circulating dendritic cells (DCs) along with reduced levels of CD4 T-cell subsets such as regulatory T cells (T_{regs}), type 1 T helper (Th1) and Th9; additionally, relative expansion of effector natural killer (NK) cells were significantly associated with severe COVID-19. Compared with patients without cancer, the levels of terminal effector CD4 T cells, T_{regs} , Th9, effector NK cells, B cells, intermediate-type monocytes and myeloid DCs were significantly lower in cancer patients with mild and severe COVID-19. We concluded that severely depleted circulating myeloid DCs and helper T subsets in the initial phase of infection were strongly associated with severe COVID-19 independent of age, type of comorbidity and other parameters. Thus, our study describes the early immune response associated with severe COVID-19 in cancer patients without intensive chemo/immunotherapy.

INTRODUCTION

Severe acute respiratory syndrome coronavirus 2 (SARS-CoV-2) infection-associated respiratory disease [coronavirus disease 2019 (COVID-19)] was declared a pandemic by the World Health Organization (WHO) on March 11, 2020.¹ With the rise of the second wave, as of May 2, 2021, a total of 211 005 326 cases of COVID-19 were diagnosed worldwide resulting in 4 419 869 deaths, thus representing the greatest public health crisis of the last few decades.² COVID-19 usually manifests with flu-like symptoms; however, a subset of patients, especially elderly patients with comorbidities, can deteriorate to severe disease (SD) with acute respiratory distress syndrome and multiorgan failure resulting in mortality.^{3–5} Several clinical trials are being conducted to treat the SD effectively, and identifying SD during the early phase of infection is essential to reduce mortality.⁶ Hence, clinically reliable biomarkers of SD during its early phase of the disease are urgently required.

S-protein and N-protein of SARS-CoV-2 have been described as the most immunogenic protein, and many studies have suggested a protective role of cell-mediated and humoral immune responses in COVID-19 infection.^{5,7–10} Recent studies have suggested the central role of cellular immune response and inflammatory cytokines in the pathogenesis of COVID-19. An association of immunological parameters, such as absolute lymphocyte count, neutrophil-to-T-cell ratio, various T-cell subsets and increased proinflammatory cytokine levels, with the clinical course of COVID-19 has also been suggested.^{3,5,6,11–14} More recently, studies have comprehensively reported the dysregulation in innate and adaptive immune responses in COVID-19.^{11,15} However, reports elaborating the immune response parameters during the early phase of infection associated with SD in cancer patients are scarce. Hence, studies describing detailed cellular immune responses in the early phase of infection, providing early insight into the host immune response and possible clinical course of disease in patients with cancer, are needed. We prospectively studied about 200 immune response parameters, including a comprehensive immune cell profile, inflammatory cytokines and other laboratory parameters, in patients diagnosed with COVID-19 in the early phase of infection and their association with SD in cancer patients without intensive chemo/immunotherapy.

RESULTS

Clinical characteristics

A total of 95 patients diagnosed with COVID-19 and 21 healthy donors (median age of 32 years, range 23–70 years) were included in this study. We included 58 (61.05%)

patients without cancer and 37 (38.95%) cancer patients without intensive chemo/immunotherapy. Details of demographical characteristics and laboratory findings are given in Table 1. The median period between COVID-19 symptoms and admission/quarantine to the hospital was 2 days (range 0–14 days). Sixty-six (69.5%) patients were admitted within the first 4 days, and all except four patients (8–14 days) within the first 7 days of COVID-19 symptoms.

At the time of admission, 89/95 (93.68%) patients were classified into nonsevere disease (NsD) (SpO₂ levels: median 98% and range 93–100%) and 6/95 (6.32%) into SD (SpO₂ levels 88–90%). Patients were reclassified into NsD ($n = 54$) and SD ($n = 41$) based on their worst WHO score during the hospital stay.^{16,17} The median time since first symptom for the first blood draw for immune monitoring was 2 days (range 0–14 days) in patients with NsD and 2.5 days (range 1–8 days) in those with SD. Notably, the median time since first day of symptom to the development of SD was 9 days (range 4–43 days).

The median age (range) for patients with NsD was 42 years (16–80 years) and for those with SD 63 years (27–84 years). Age over 59 years (receiver operating characteristic-based cut-off) was strongly associated with SD [odds ratio (OR) 16.23; $P < 0.0001$]. Frequency of SD in patients with comorbidities, including cancer, was high (50.7% versus 22.2%; OR 4.62, $P = 0.01$). There was no difference in SD frequency between patients with hematological and nonhematological cancer ($P = 0.1$). The median duration of follow-up was 31 days (range 4–92 days). The median time since admission to the hospital for developing SD was 5 days (range 1–17 days). Of the 41 patients with SD, 18 recovered from COVID-19, but 23/41 (56%) patients succumbed to acute respiratory distress syndrome.

Immune cell landscape

We studied absolute counts of immune cell subsets and their relative proportions in the respective compartments. Collectively, 175 immune cell parameters derived from 69 immune cell subsets were studied. Details of immune cell perturbations in COVID-19 patients (with or without cancer) compared with healthy donors are given in Supplementary table 1 (Figures 1–3). The details of sensitivity, specificity and OR of the absolute counts of the most significant immune cell parameters with area under the curve of 0.75 or higher are given in Table 2 (Supplementary tables 1 and 2).

Immune perturbations: nonsevere versus severe COVID-19 patients

We studied 200 parameters, including age, immune cell subsets, cytokine levels and other laboratory parameters

Table 1. Baseline demographic and clinical characteristics of patients with COVID-19

Characteristics	Total (n = 95)	Nonsevere disease (n = 54)	Severe disease (n = 41)
Age (years), median (range)	52 (16–84)	41.5 (16–80)	63 (27–84)
Sex, n (%)			
Male	57 (60)	34 (63)	23 (56.1)
Female	38 (40)	20 (37)	18 (43.9)
Duration since first symptom and admission to hospital			
Median (range) in days	2 (0–14)	2 (0–14)	2.5 (1–7)
Duration between diagnosis and admission to hospital			
Median (range) in days	0.5 (0–13)	1 (0–13)	0.5 (0–7)
Duration since first symptom to severe disease			
Median (range) in days	—	—	8 (4–43)
Comorbidities, n (%)			
Total	73 (69.4)	36 (68.5)	37 (35.2)
Hematological cancer	17 (16.2)	11 (10.4)	6 (05.7)
Nonhematological cancer	20 (19.0)	8 (7.6)	12 (11.4)
Diabetes	23 (21.9)	9 (16.7)	14 (34.1)
Hypertension	26 (24.7)	9 (18.5)	16 (39.0)
Chronic pulmonary disease	4 (3.8)	1 (1.9)	3 (7.3)
Other	1 (1.9)	1 (1.9)	1 (2.4)
Two or more comorbidities	19 (18.1)	10 (18.1)	9 (22.0)
Clinical symptoms and signs at diagnosis, n (%)			
Fever	87 (91.6)	47 (87.0)	40 (97.6)
Cough	57 (60.0)	26 (48.1)	31 (75.6)
Sore throat	72 (75.8)	33 (61.1)	39 (95.1)
Headache	57 (51.6)	25 (46.3)	24 (58.5)
Myalgia	56 (58.9)	23 (42.6)	33 (80.5)
Rhinitis/Rhinorrhea	33 (34.7)	22 (40.7)	31 (75.6)
Loss of taste or smell	29 (30.5)	14 (25.9)	15 (36.6)
Nausea or vomiting	19 (18.1)	06 (11.1)	11 (26.8)
Baseline RT-PCR C _t values, median (range)			
E gene	18.7 (10.4–36)	21.5 (10.4–36)	21.3 (13.3–32)
RdRp gene	22.5 (9.7–36.6)	22.0 (9.7–33.4)	20.4 (14.8–36.5)
SpO ₂ levels			
Median (range) % at admission	98 (70–100)	98 (96–100)	97 (70–100)
Median (range) % at worst score	97 (92–100)	98 (95–100)	80 (40–94)
WHO score			
Median (range) at admission	3 (2–6)	3 (2–3)	3 (2–5)
Median (range) at worst score	3 (2–8)	3 (2–4)	7 (5–8)
Blood counts at diagnosis, median (range)			
Hb (g mL ⁻¹)	120 (45–159)	129 (61–159)	107 (45–154)
White blood cells ($\times 10^9$ L ⁻¹)	5.31 (0.32–28.7)	4.59 (0.32–16.7)	9.9 (1–28.7)
Platelet ($\times 10^9$ L ⁻¹)	208 (19–472)	198 (50–444)	215 (19–472)
Coagulation profile at diagnosis ^a			
PT (s)	16 (13–149)	15 (14–19)	16 (13–149)
aPTT (s)	32 (20–60)	33 (25–60)	31 (20–46)
INR	1.0 (0.9–2.0)	0.9 (0.9–1.28)	0.99 (0.9–2.0)
Fibrinogen (mg dL ⁻¹)	342 (143–810)	297(185–803)	458 (143–810)
Other laboratory parameters at diagnosis ^a			
C-reactive protein (mg%)	2 (0.1–48)	0.7 (0.1–14.4)	9.7 (0.1–48)
Procalcitonin (ng mL ⁻¹)	0.0 (0.0–59.8)	0.05 (0.05–0.48)	0.13 (0.05–59.8)

aPTT, activated partial thromboplastin time; Hb, hemoglobin; INR, international normalized ratio; PT, prothrombin time; RT, reverse transcriptase; WHO, World Health Organization.

^aThese tests were available in 65 patients (nonsevere = 41, severe = 24).

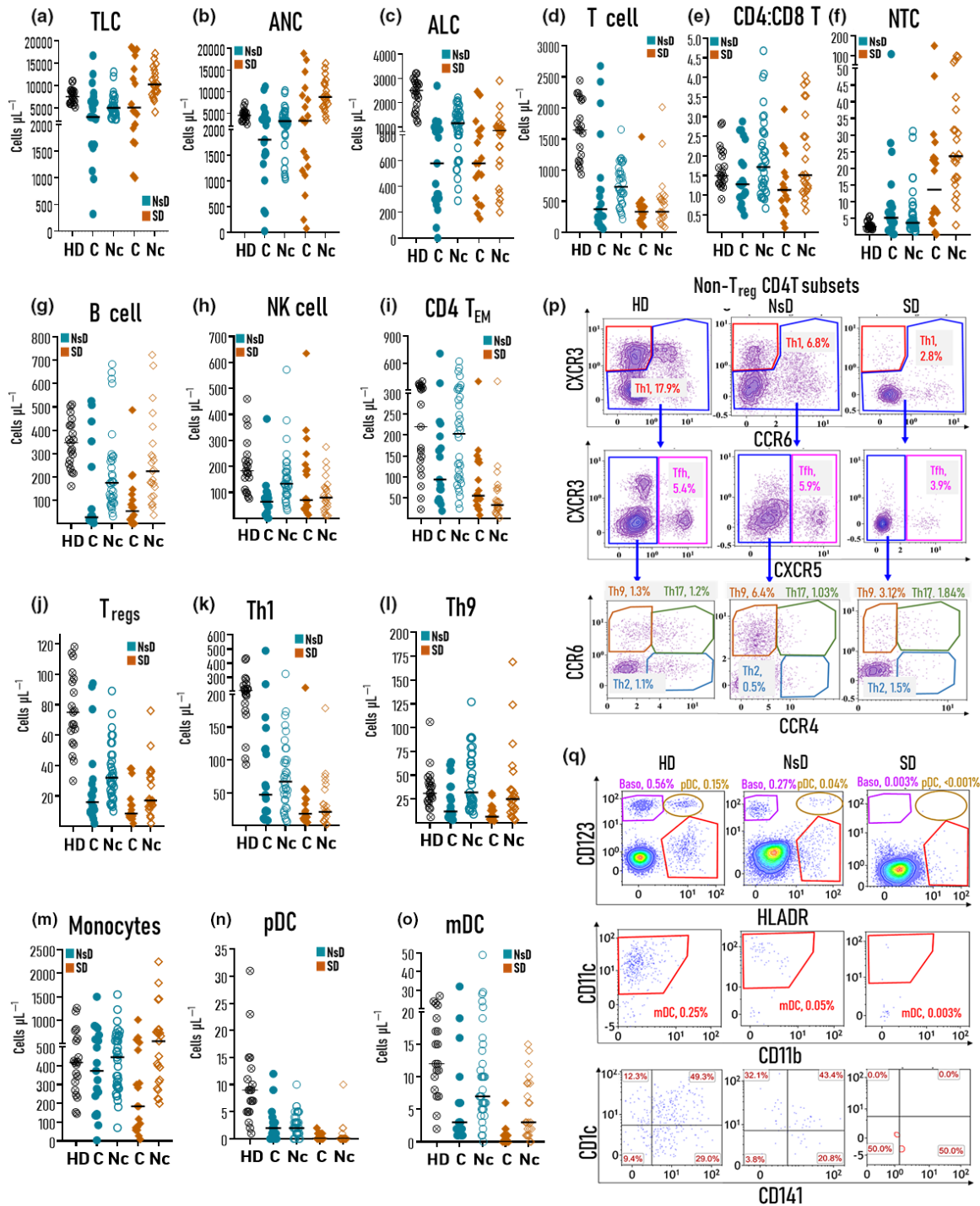


Figure 1. The levels of various immune cell subsets in a healthy donor (HD; $n = 21$), in patients with nonsevere COVID-19 (NsD; $n = 54$) and in patients with severe COVID-19 (SD; $n = 41$). Patients with cancer are indicated with “C” ($n = 37$) and without cancer with “Nc” ($n = 58$). **(a–c)** The distribution of complete cell count parameters in healthy donors and COVID-19 patients. **(d–o)** The distribution of important immune cell subsets in healthy donors and COVID-19 patients. **(p)** Representative flow cytometry plots depicting the gating strategy for key CD4 T-cell subsets (Th1, Th2, Th9, Th17 and Tfh) after exclusion of T-regulatory cells. **(q)** Representative flow cytometry plots depicting the gating strategy for identifying basophils and dendritic cell subsets. ALC, absolute lymphocyte count; ANC, absolute neutrophil count; Baso, basophil; COVID-19, coronavirus disease 2019; EM, effector memory; fh, follicular helper; mDC, myeloid dendritic cell; Nc, nonclassical; NsD, nonsevere disease; NTC, neutrophil-to-T-cell ratio; pDC, plasmacytoid dendritic cell; reg, regulatory; SD, stable disease; Th, T helper cell; TLC, total leukocyte count.

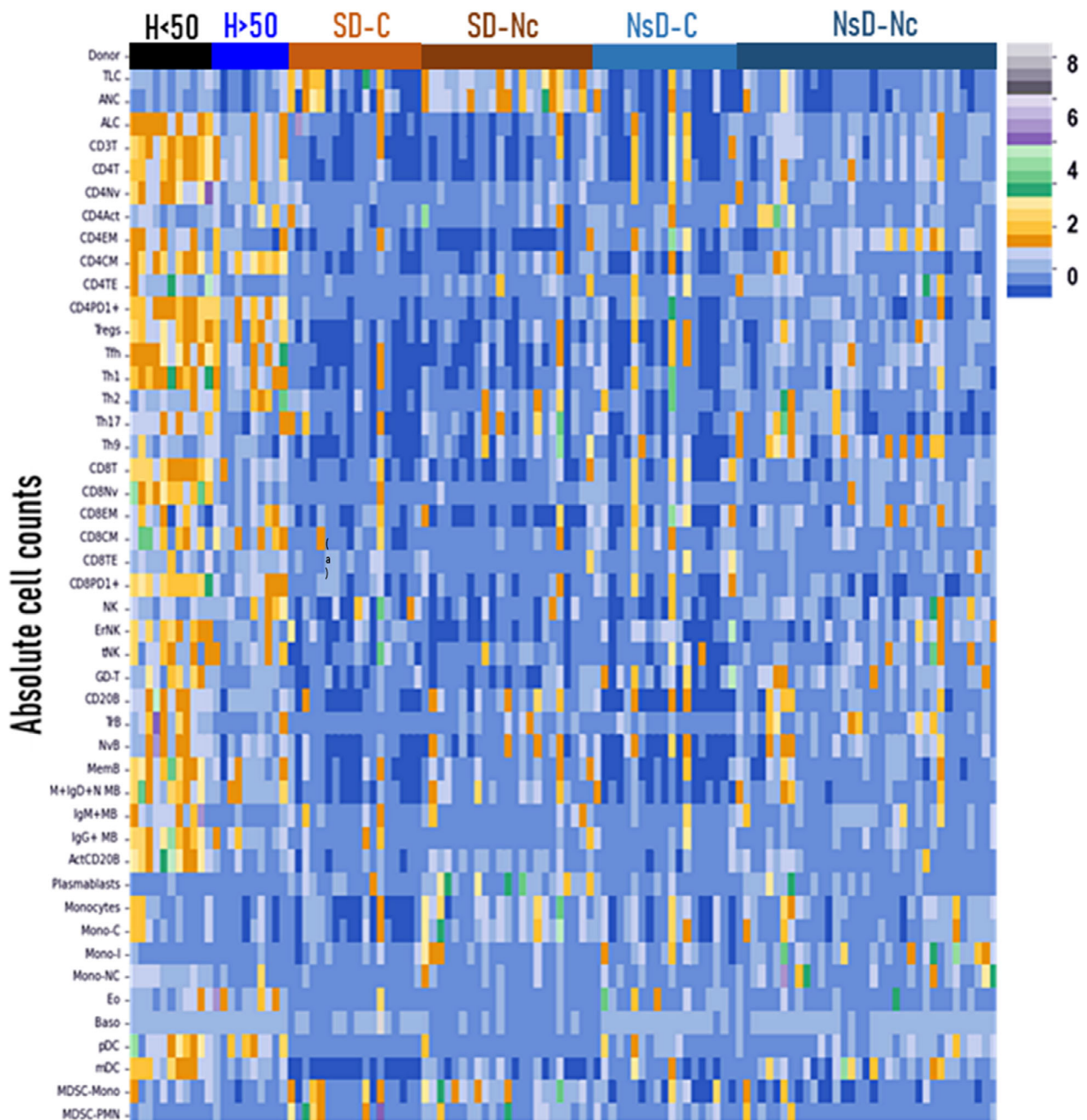


Figure 2. Heatmap showing absolute counts of various statistically relevant immune cell subsets in healthy donors and COVID-19 patients. Each row in the heatmap represents an immune cell parameter, and each column represents a patient. The scale is normalized for each parameter. Patients with cancer are indicated with "C" ($n = 37$), without cancer with "Nc" ($n = 58$), healthy donors with "H" (H < 50, i.e. age < 50 years; $n = 11$ and H > 50, i.e. age ≥ 50 years; $n = 10$), nonsevere disease with "NsD" ($n = 54$) and severe disease with "SD" ($n = 41$). Act, activated; ALC, absolute lymphocyte count; ANC, absolute neutrophil count; B, B cell; Baso, basophils; C, classical; CM, central memory; COVID-19, coronavirus disease 2019; cPC, circulating plasma cell (plasmablasts); Eff, effector; EM, effector memory; Eo, eosinophil; Er, early; Exh, exhausted (PD1⁺ T cells); fh, follicular helper; GD, $\gamma\delta$ T cells; I, intermediate; mDC, myeloid dendritic cell; MDSC, myeloid-derived suppressor cell; Mem, memory; Mono, monocytic; Nc, nonclassical; NsD, nonsevere disease; NTC, neutrophil-to-T-cell ratio; NtM, natural memory; NV, naïve; pDC, plasmacytoid dendritic cell; PMN, polymorphonuclear; reg, regulatory; SD, stable disease; T, T cells; t, terminal; TE, terminal effector; TLC, total leukocyte count; Tr, transitional.

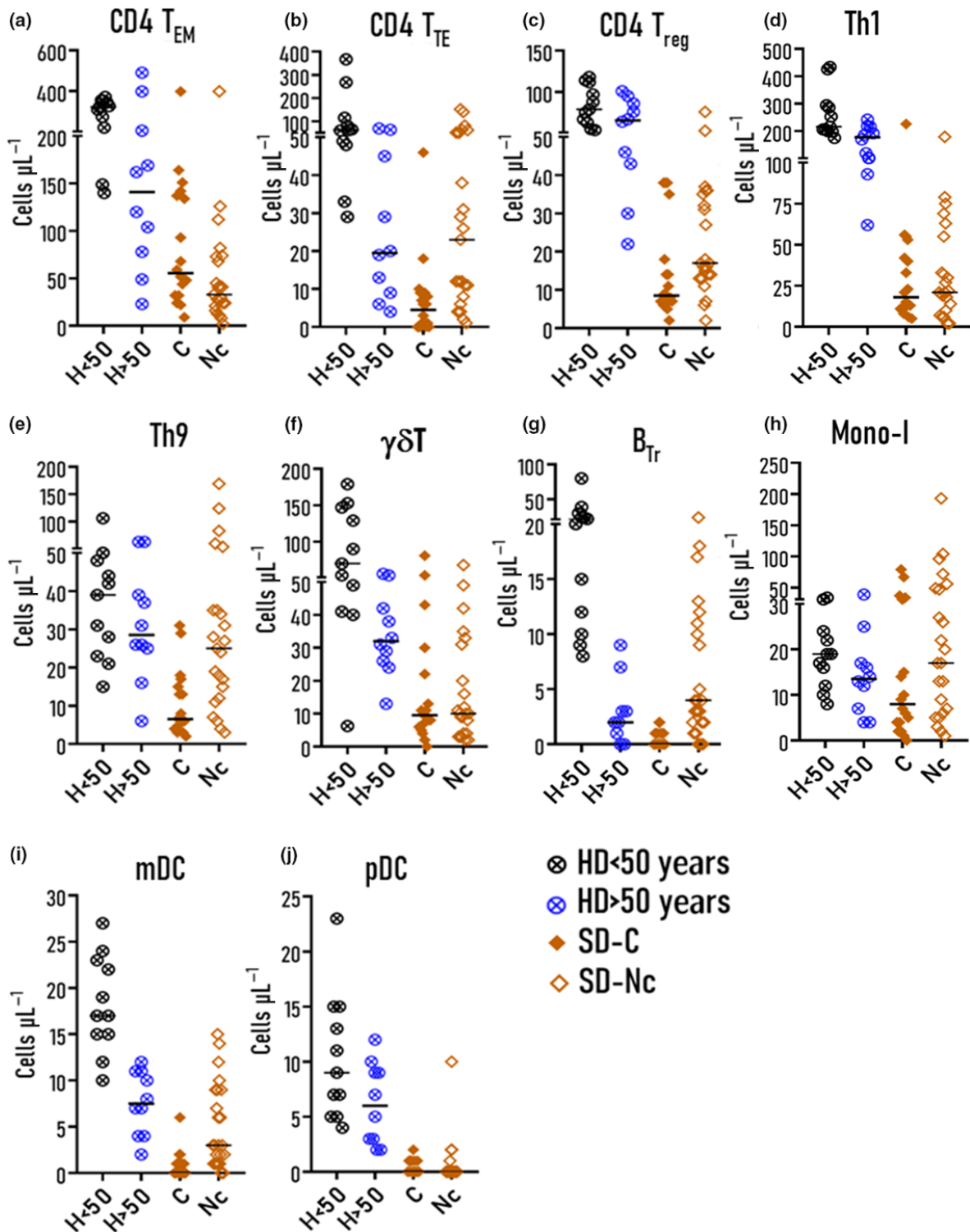


Figure 3. The levels of absolute counts of statistically relevant immune cell subsets demonstrating the comparison between severe COVID-19 in patients with cancer (C, $n = 18$) and without cancer (C, $n = 23$) as well as age-wise categorized healthy donors. Healthy donors with age under 50 years are indicated with H < 50 ($n = 11$) and those aged 50 years or older are indicated with H > 50 years ($n = 10$). (a–e) The distribution of CD4 T-cell subsets in age-matched healthy donors and patients (cancer and non-cancer) with severe COVID-19. The distribution of $\gamma\delta\text{T}$ -cells (f), transitional B cells (g), intermediate-type monocytes (h), conventional (myeloid) dendritic cells (i) and plasmacytoid dendritic cells (j) in age-matched healthy donors and patients (cancer and non-cancer) with severe COVID-19. B, B cell; B_{Tr}, transitional B cells; C, classical; EM, effector memory; HD, healthy donor; I, intermediate; mDC, myeloid dendritic cell; mono, monocyte; Nc, nonclassical; NsD, nonsevere disease; pDC, plasmacytoid dendritic cell; SD, stable disease; T, T cell; TE, terminal effector; Th, T helper cell; Tr, transitional; T_{reg}, regulatory T cell.

Table 2. Levels of the most significant immune cell subsets of COVID-19 patients

Immune cell subset	Disease status		Association with severe COVID-19				
	Nonsevere (n = 54)	Severe (n = 41)	Cut-off criteria ^a	Sensitivity (95% CI)	Specificity (95% CI)	Odds ratio (95% CI)	BH-adjusted P-value
Absolute cell counts (μL^{-1}), median (range)							
CD4 T _{EM}	156 (19–992)	44 (2–399)	≤ 68	68.29 (51.90–81.90)	81.48 (68.60–90.70)	9.47 (3.66–24.53)	0.0001
CD4 T _{TE}	18 (0–249)	9 (0–152)	≤ 12	65.85 (49.40–79.90)	57.41 (43.20–70.80)	2.81 (1.21–6.52)	0.0165
T _{regs}	28 (2–94)	14 (2–76)	≤ 18	68.29 (51.90–81.90)	68.52 (54.40–80.50)	4.68 (1.96–11.23)	0.0006
Th1	61 (6–488)	21 (2–226)	≤ 33	70.73 (54.50–83.90)	70.37 (56.40–82.00)	5.74 (2.35–13.99)	0.0001
Th9	25 (3–127)	15 (2–169)	≤ 35	87.80 (73.80–95.90)	40.74 (27.60–55.00)	4.95 (1.68–14.60)	0.0038
B _{Tr}	4 (0–47)	1 (0–24)	≤ 2	63.41 (46.90–77.90)	66.67 (52.50–78.90)	3.77 (1.60–8.88)	0.0026
$\gamma\delta$ -T	38 (1–277)	10 (0–81)	≤ 13	68.29 (51.90–81.90)	74.07 (60.30–85.00)	6.15 (2.51–15.08)	0.0001
Mono-I	37 (0–293)	13 (0–193)	≤ 15	56.10 (39.70–71.50)	83.33 (70.70–92.10)	6.39 (2.48–16.43)	0.0001
pDC	2 (0–12)	0 (0–10)	≤ 1	90.24 (76.90–97.30)	66.67 (52.50–78.90)	6.28 (2.56–15.43)	0.0001
mDC	6 (0–49)	1 (0–15)	≤ 3	75.17 (57.10–85.80)	78.52 (54.40–80.50)	15.16 (5.30–43.39)	0.0001
CD141 ⁺ mDC ^b	4 (0–32)	0 (0–5)	≤ 1	83.33 (62.60–95.30)	78.05 (62.40–89.40)	26.92 (6.71–107.90)	0.0001
CD1c ⁻ CD141 ⁻ mDC ^b	1 (0–26)	0 (0–1)	≤ 0	91.67 (73.00–99.00)	56.10 (39.70–71.50)	5.81 (1.79–18.87)	0.0035

BH, Benjamini–Hochberg correction; B_{Tr}, transitional B cells; C, classical; CI, confidence interval; CM, central memory; Eff, effector; EM, effector memory; I, intermediate; mDC, myeloid dendritic cell; mono, monocytes; NC, nonclassical; pDC, plasmacytoid dendritic cell; reg, regulatory; Th, T helper cell; T_{regs}, regulatory T cells; T_{TE}, terminal effector CD4 T cell.

^aCut-off criteria were defined using ROC analysis.

^bData were available in only 65 patients.

(Supplementary table 1). A total of 79 parameters were found to be associated with severe COVID-19. The top 25 parameters demonstrating a strong association with the SD (area under the curve > 0.75) were analyzed further. Patients with severe COVID-19 predominantly belonged to the elderly age group. Hence, the levels of immune cell parameters significantly associated with SD were also compared with levels of age-adjusted healthy donors (median age 62 years, range 51–70 years) as shown in Table 3 and Figures 2 and 3.

Adaptive immune response compartment. In accordance with previous reports, our data also revealed a significant association of reduced CD3 T, CD4 T, CD8 T cells and transitional B cells, and increased neutrophil-to-T-cell ratio and plasmablasts count with SD (Figures 1d–h and 2).^{5,7,8,15,18,19} Our data distinctly highlighted that within CD4 T-cell subsets, the decreased counts of effector memory CD4 T-cell (CD4 T_{EM}), CD45 RA⁺ terminal effector CD4 T cell (CD4 T_{TE}), T_{regs}, type 1 T helper (Th1) and Th9 were associated with severe COVID-19 (Figure 1i–l and Table 2). In cytotoxic T-cell subsets, in addition to previously reported increased proportion of activated CD8 T cells, the reduced counts of naïve-CD8 T (CD8 T_{NV}), CD94⁺ $\gamma\delta$ T and CD69⁺ $\gamma\delta$ T cells were found to be associated with SD (Supplementary table 1).^{11,12} Within the natural killer (NK) cells, an expanded proportion of effector NK cell (NK_{eff}) subset was associated with SD (Supplementary table 2).

Innate immune response compartment. As reported previously, we also observed an association of higher levels of absolute neutrophil count and reduced levels of monocytes (classical, intermediate and nonclassical), eosinophils and basophils with SD (Supplementary tables 1 and 2).^{5,8,11,13,15,18,20,21} By contrast, increased myeloid-derived suppressor cells monocyte type percentages in total leukocyte counts showed a tendency toward SD.

Notably, in the dendritic cell (DC) compartment, decreased levels of myeloid DCs (mDCs) showed a strong association with SD (absolute $\leq 3 \mu\text{L}^{-1}$; OR 15.2, $P = 0.0001$ and percentages $\leq 0.05\%$; OR 27.9, $P = 0.0001$). Likewise, reduced plasmacytoid DC levels were also associated with SD (absolute $\leq 1 \mu\text{L}^{-1}$; OR 6.28, $P = 0.0001$ and percentages $\leq 0.03\%$; OR 17.04, $P = 0.0001$) (Table 2 and Supplementary table 2).

Immune perturbations: cancer versus noncancer comorbidities

As comorbidities such as cancer can also result in immune dysregulation,^{21,22} we compared the levels of immune cell parameters significantly associated with severe COVID-19 (area under the curve > 0.75) between the age-matched patients with and without cancer (Figures 1 and 3 and Table 3, Supplementary table 3). The levels of CD4 T_{TE}, T_{regs}, Th9 cells, intermediate-type monocytes and mDC, and proportion of the NK_{eff} subset within NK cells were significantly lower in cancer patients with NsD and SD

Table 3. The distribution of statistically significant immune cell subset levels in COVID-19 patients with and without cancer

Immune cell subset	Nonsevere disease			Severe disease		
	Cancer (<i>n</i> = 19)	Noncancer (<i>n</i> = 35)	BH-adjusted <i>P</i> -value	Cancer (<i>n</i> = 18)	Noncancer (<i>n</i> = 23)	BH-adjusted <i>P</i> -value
Absolute cell counts (μL^{-1}), median (range)						
CD4 T _{EM}	94 (19–992)	203 (25–621)	0.1640	55 (9–398)	33 (2–399)	0.1483
CD4 T _{TE}	3 (0–234)	32 (2–249)	0.0078	4 (0–46)	23 (1–152)	0.0024
T _{regs}	16 (2–94)	32 (10–89)	0.0454	9 (2–38)	17 (2–76)	0.1510
Th1	47 (8–488)	67 (6–324)	0.5490	18 (5–226)	21 (2–179)	0.8604
Th9	12 (3–64)	32 (9–127)	0.0056	7 (2–31)	25 (3–169)	0.0077
B _{Tr}	0 (0–17)	6 (0–47)	0.0048	0 (0–2)	4 (0–24)	0.0016
$\gamma\delta$ -T	33 (1–277)	38 (7–106)	0.5301	10 (0–81)	10 (2–68)	0.9686
Mono-I	27 (0–140)	40 (4–293)	0.5051	8 (0–79)	17 (1–193)	0.2981
mDC	3 (1–32)	7 (0–49)	0.0345	0 (0–6)	3 (0–15)	0.0016
pDC	2 (0–12)	2 (0–10)	0.5051	0 (0–2)	0 (0–10)	0.4354

BH, Benjamini–Hochberg correction; B_{Tr}, transitional B cells; C, classical; CM, central memory; Eff, effector; EM, effector memory; I, intermediate; mDC, myeloid dendritic cell; mono, monocyte; NC, nonclassical; pDC, plasmacytoid dendritic cell; reg, regulatory; Th, T helper cell; T_{regs}, regulatory T cells; T_{TE}, terminal effector CD4 T cell.

compared with the corresponding groups of patients without cancer (Figure 3 and Table 3). By contrast, the levels of CD4 T_{EM} were slightly higher in cancer patients with NsD. We also noted significantly lower B-cell levels in cancer patients than noncancer patients independent of the severity of COVID-19 (Figure 1g).

Inflammatory cytokines and other laboratory parameters

Data on inflammatory cytokines and laboratory parameters such as coagulation profile, C-reactive protein and procalcitonin were available in only 65 patients (NsD=41 and SD=24) and are given in Supplementary table 1. Among the cytokines studied, an increased level of interleukin-6 (IL-6; $\geq 40 \text{ pg } \mu\text{L}^{-1}$) was found to be highly specific (95.12%), and IL-10 ($\geq 2.7 \text{ pg } \mu\text{L}^{-1}$) was found to be a highly sensitive (95.83%) biomarker of SD. Increased C-reactive protein, procalcitonin and fibrinogen levels were associated with SD within routine hematological and biochemical parameters.

Multivariate analysis

We also performed multivariate analysis using the top 25 parameters demonstrating a strong association with SD with a high area under the curve (> 0.75 ; Table 2 and Supplementary table 2). These 25 parameters included age, immune cell subsets and cytokines IL-6 and IL-10. On multiple logistic regression analysis of parameters with variance inflation factor < 6 , the markedly reduced levels of mDC ($P < 0.0001$) was the only parameter that

was found to be independently associated with SD (independent of factors that included age, type of comorbidity, lymphocyte subsets and cytokines such as IL-6 and IL-10).

Developing immune signatures using principal component analysis

Using immune parameters associated with COVID-19, the unsupervised principal component analysis revealed three distinct immune signatures (ISs; Supplementary figure 2). Briefly, “type 1 IS” ($n = 14$, SD = 7 patients, NsD = 7 patients) was characterized by activation of immune cells and demonstrated CD8 $>$ CD4, increased CD8 T_{EM}, CD8 T_{TE}, CD38⁺HLADR⁺ T_{Act} cells, CD69⁺ activated NK (NK_{Act}) cells, B_{Act} cells and plasmablasts. This IS represented overt activation of the innate and adaptive immune response, but interestingly, it included mixed cases of SD and NsD. “Type 2 IS” ($n = 33$, SD = 25 and NsD = 8) was characterized by (i) increased levels of absolute neutrophil count, Th2, Th17, PD1⁺ T and NK_{eff}, CD4 $>$ CD8; (2) decreased proportion of Th1, Th9, $\gamma\delta$ T cells, monocytes (especially, the intermediate type), mDC and plasmacytoid DC and (3) elevated levels of IL-6 and IL-10. Thus, IS-2 was predominantly composed of patients with SD. “Lastly, the “type 3 IS” ($n = 48$, NsD predominant, NsD = 39, SD = 9) was characterized by CD4 $>$ CD8; normal levels of Th1, Th9, follicular helper T cells, CD4 T_{EM} and CD4 T_{TE}; a proliferation of IgM⁺IgD⁺ B_{NV} cells and normal levels of DC as well as IL-6 and IL-10. There was no a significant difference between the time since symptom onset of

COVID in patients with these three ISs ($P > 0.2$). Thus, type 1 IS included mixed patients, type 2 IS was predominantly composed of SD and type 3 IS of NsD. The median (range) time since first symptom of COVID-19 for IS-1, IS-2 and IS-3 were 3 days (2–14 days), 3 days (1–9 days) and 2.5 days (0–7 days), respectively.

DISCUSSION

Recent studies have demonstrated the clinical features, standard laboratory parameters and immunological dysregulations in cancer patients with active disease or on active chemotherapy/immunotherapy.^{21–25} These studies highlighted the ISs and seroconversions during acute infection or at later time points. The focus of this study was to study the different aspects of the early immune response between nonsevere and severe COVID-19 in cancer patients without intensive chemo/immunotherapy. We studied immune perturbations, particularly during the early phase of infection, and evaluated their association with severe COVID-19 in patients with and without cancer.

Similar to previously published reports, our results showed an association of depletion in T-cell subsets, increased neutrophil-to-T-cell ratio, a higher proportion of activated/exhausted CD8 T cells and increased levels of plasmablasts with SD.^{3,11,15,18,20} Our results distinctly highlighted the strong association of decreased levels of CD4 T_{EM}, T_{reg}, Th1 and Th9 cells with severe COVID-19. CD4 T cells play a central role in orchestrating immune responses; Th1 cells promote cytotoxic mechanisms by activating CD8 T cells with interferon- γ and simultaneously stimulate B-cell responses facilitating viral-specific humoral responses.⁷ Similarly, Th9 cells interact with innate cells such as mast cells and basophils through IL-9 initiating inflammation, especially in the pulmonary and nervous systems.²⁶ By contrast, T_{regs} are mainly responsible for immune suppression.^{7,27} Reduced levels of these circulating CD4 T subsets reflect a marked dysregulation of immune responses probably because of either decreased production or increased recruitment to the primary site in COVID-19 progressing to SD.

In addition to the depletion of monocytes, eosinophils and basophils within the innate immune cell compartment, our results pointed out the strong association between the marked reduction of circulating DCs and progression to severe COVID-19. Recent studies have also documented the association of decreased DC levels with severe COVID-19. Still, they are predominantly limited to noncancer patients with acute infection.^{11,20,27,28} In the present study, we documented the immune dysregulations during the early phase of infection when most of the patients were categorized into

NsD, thereby highlighting its association with progression to SD.

Further, we compared the immune cell deviations between COVID-19 patients with and without cancer. We observed that the levels of CD4 T_{TE}, T_{regs}, Th9 cells, NK_{eff} cells, B cells, intermediate-type monocytes and mDC were significantly lower in cancer patients with mild as well as severe COVID-19 than in the corresponding group of patients without cancer. These findings substantiate pre-existing immune dysregulation in cancer patients resulting in lower baseline levels of immune cell subsets in these patients compared with age-matched healthy individuals, as reported recently.²¹

Notably, our data documented an independent association (independent of age, comorbidities and other parameters) between marked depletion of circulating mDCs in the early phase of infection and severe COVID-19 on multivariate analysis. This indicates a key role of DCs in the early immune response associated with severe COVID-19. DCs, indeed, play a major role in the innate and adaptive immune system and are the most effective antigen-presenting cells.²⁹ They recognize viral antigens through Toll-like receptors, migrate to lymphoid organs and initiate a specific immune response.²⁹ An acute viral infection induces DC activation, followed by migration of DCs from peripheral blood to the tissue with infection (such as lungs), leading to depletion in the circulating DC levels.³⁰ Recent studies have documented the reduced levels of circulating DCs during the acute phase of SARS-CoV-2 infection.^{20,27,28} Moreover, studies involving autopsies and bronchoalveolar lavage analysis in COVID-19 patients have provided conclusive evidence on the central role of DCs in the immunopathogenesis of COVID-19.^{18,19,28} These reports and the results of our study emphasize that the markedly reduced levels of mDCs and plasmacytoid DCs in peripheral blood during the initial phase of infection can provide an early indicator of SD and offer a useful biomarker for COVID-19 monitoring in patients with comorbidities such as cancer.

Furthermore, the unsupervised principal component analysis revealed three distinct ISs. The first group (IS-1) was dominated with a higher proportion of activated T cells and included mixed severe and nonsevere patients. The second group (IS-2) was dominated by depleted innate and adaptive immune cells and mainly composed of patients with SD. The third group (IS-3) demonstrated the immune response close to the healthy donors lacking the other two immune responses. Interestingly, a previously published report also observed three types of immune responses (immunotypes 1, 2 and 3) using Uniform Manifold Approximation and Projection (UMAP)-based clustering.¹¹ We observed a significant

overlap between IS-1 and IS-3 from our data and their immunotype-1 and immunotype-3 signatures. However, we could not relate the IS-2 signature to any of the immunotypes observed in this report,¹¹ which could be because of the absence of proliferation studies in our data or the use of only mononuclear cell proportions (not absolute counts) by them.

Our study was limited to a small cohort of patients. The cut-off thresholds derived for different immune cell subsets in this data set may not provide equal sensitivity and specificity to other trials. Studies with a larger cohort may offer reproducible thresholds. Besides, a common challenge for the broader clinical application of these immune parameters is the scarcity of clinical flow cytometry laboratories and limited expertise. It is still away from becoming a part of the routine investigations in infectious diseases, especially in resource-limited regions.

In summary, we performed an in-depth immune response profiling during the early phase of COVID-19 in patients with nonactive cancer. Our data revealed a characteristic immune profile that can provide an additional effective tool for high-risk assessment in patients with COVID-19 during the early phase of infection. Our results suggested that monitoring the levels of peripheral blood CD4 T-cell subsets and DCs in the early phase of infection provides valuable insight into the host immune response and understanding of the possible clinical outcome of COVID-19 in cancer patients.

METHODS

Patients

We prospectively studied the consecutive patients diagnosed with COVID-19 infection admitted or quarantined by our hospital (a tertiary referral cancer center). The study was approved by the Institutional Ethical Committee. Diagnosis of COVID-19 was confirmed with SARS-CoV-2-specific real-time reverse transcription-PCR. The study included two groups of COVID-19 patients: (i) cancer patients who were getting treated in our cancer specialty hospital and (ii) symptomatic hospital staff and/or their relatives with COVID-19 infection who were either hospitalized for clinical care or quarantined in the hospital facility (because of a lack of a home quarantine facility). Of note, asymptomatic patients or staff were not included in the study. Informed consent was obtained from all participants of the study. Because active cancer and intensive chemotherapy can significantly impact patients' immune systems, we included only those cancer patients who had either stopped chemotherapy for more than 3 months or were on maintenance therapy only. The cancer patients receiving monoclonal antibody therapy, induction/consolidation phase chemotherapy, post-transplantation patients and patients with white blood cell or absolute lymphocyte count counts lower than normal limits in the last 2 months before COVID-19 infection were excluded from

this study. The COVID-19 infection status was evaluated using a "WHO 8-point scale" until discharge from the hospital.^{16,17} Patients with a WHO score of 5 or more with clinical signs of pneumonia plus either oxygen saturation (SpO₂) levels less than 90% or SpO₂ levels between 90% and 94% but respiratory rate over 30 min⁻¹ requiring high-flow supplemental oxygen (≥ 15 L min⁻¹) were categorized as having SD.¹⁶ The remaining patients with a WHO score less than 5 were categorized as having NsD. Patients were followed up either until they became negative for SARS-CoV-2 or died because of the disease. The immune response evaluation, including immune cell profile, cytokines and other parameters, was studied in blood samples collected within 12 h of admission or quarantine.

Real-time reverse transcription-polymerase chain reaction

A nasal and oropharyngeal swab was collected in molecular transportation media (Huwel Lifesciences Pvt Ltd, Hyderabad, Telangana, India). Viral total nucleic acid was extracted using the QIAamp MinElute Virus Spin kit (Qiagen, Hilden, Germany). SARS-CoV-2 positivity was detected by real-time reverse transcriptase-PCR using PathoDetect™ COVID-19 Qualitative PCR kit (Mylab Discovery Solutions, Lonavala, Maharashtra, India). Real-time reverse transcriptase-PCR steps were as follows: 50°C for 15 min of preincubation and 95°C for 20 s for initial denaturation followed by 45 cycles of amplification at 95°C for 5 s and 58°C for 30 s. Cycle threshold (C_t) ≤ 40 was taken as positive. The positive SARS-CoV-2 real-time reverse transcriptase-PCR result was defined if both *E* and *RdRP* genes were detected.

Cytokine profile analysis

Cytokine profile analysis for IL-1 β , IL-6, IL-8, IL-10 and IL-12p17 was performed using the patient's peripheral blood plasma samples (within 4 h of collection) using a cytometric bead array (BD Biosciences, San Jose, CA, USA) according to manufacturer's instructions. In brief, 50 μ L of prepared capture bead mixture was mixed with 50 μ L of the diluted sample and incubated at room temperature for 1.5 h. Then, 50 μ L of the detection reagent was added to this mixture and incubated for 1.5 h. The detection reagent is a mixture of analyte-specific antibodies conjugated to phycoerythrin. Incubation of the samples with capture beads and then the detection reagent leads to the formation of a "sandwich complex" of the three. These complexes were acquired on LSRFortessa (BD Biosciences), and data were analyzed using FCAP Array software (BD Biosciences).

Flow cytometric characterization of immune cell profile

Immune cell profile was studied on fresh whole blood samples with a comprehensive 14–16-color antibody panel (Supplementary table 4) using the stain–lyse–wash method. In brief, the peripheral blood sample was incubated with a pretitered volume of antibody cocktails for 20 min at room temperature

in the dark. For B-cell antibody panel staining, the cells were subjected to two washes at 540g for 2 min with a BD Sheath reagent (BD Biosciences) before staining the sample. This was followed by red cell lysis using OptiLyse C Lysis Solution (Beckman Coulter, Inc., Miami, FL, USA) for 10 min at room temperature in the dark. Antibodies used against the markers (Supplementary table 4) were CD1c, CD3, CD4, CD5, CD7, CD8, CD10, CD11b, CD11c, CD14, CD16, CD19, CD20, CD25, CD27, CD28, CD33, CD38, CD45, CD45RA, CD56, CD64, CD69, CD83, CD94, CD95, CD123, CD127, CD141, CD183, CD185, CD194, CD196, CD197, CD274, CD279, CD370, TCR $\gamma\delta$, HLA-DR, immunoglobulin (Ig) M, IgD and IgG. The cells were acquired on an LSRFortessa flow cytometer (BD Biosciences), and a minimum of 100 000 cells were studied in each tube. In samples with lower counts (< 1000 white blood cells μL^{-1}), up to 300 000 events per tube were studied. The limit of detection of “20 events” using samples from healthy donors was applied to include any immune cell subset for further analysis. Flow cytometry data were analyzed using a pre-designed template-based conventional approach using Kaluza software (version 2.1; Beckman Coulter, Inc.). The gating strategy used to identify various immune cell subsets was adopted from previously published reports (described in the Supplementary figure 1).^{31,32} Absolute cell counts were determined using a dual-platform strategy.³³ Total leukocyte counts were determined from complete cell counts on an automated hematology analyzer (Advia2120i), and absolute counts for each parameter were calculated by multiplying percentages of cells in total CD45⁺ cells with total leukocyte counts/100.

Gating strategy

The gating strategy (Supplementary figure 1) used to identify immune cell subsets was developed based on the recently published reports.^{32,34–37} All major immune cell subset counts were determined using the first antibody combination (as given in Supplementary table 4). This was followed by measurement of CD4 and CD8 T-cell subsets (naïve, memory, effector, activated, exhausted) and helper CD4 T-cell subsets (CD127⁻CD25⁺ T_{regs}, CXCR3⁺CCR4⁻CCR6⁻ Th1, CXCR3⁻CCR4⁺CCR6⁻ Th2, CXCR3^{+/-}CCR4⁻CCR6⁺ TH9, CXCR3⁻CCR4⁺CCR6⁺ Th17 and CXCR5⁺ follicular helper T cells) using the second antibody combination as described previously.^{32,34,38} B-cell subsets (transitional, naïve, memory, activated, plasmablasts) were determined using the third combination. NK cell subsets (early, effector, terminal, CD69⁺, CD94⁺) and $\gamma\delta$ T-cell subsets (naïve, memory, activated) were determined using the fourth combination. Lastly, quantitation of subsets of monocytes (classical, intermediate, nonclassical), mDCs (CD1c⁺CD141⁻, CD1c⁺CD141⁺, CD1c⁻CD141⁻, CD1c⁻CD141⁺), plasmacytoid DCs, eosinophils, basophils and myeloid-derived suppressor cell subsets (monocytic and polymorphonuclear type) was accomplished by the fifth combination using gating approaches described previously (Supplementary figure 1).^{22,31,32,35,39,40}

Principal component analysis. The proportion of various immune subsets generated from all tubes was further utilized

to perform principal component analysis using the prcomp function in Rv4.0.2, and k-means clustering was used to generate relevant clusters.

Statistical analysis

The quantitative differences in the immune cell subsets between healthy donors and COVID-19 patients and between patients with and without cancer were evaluated using the Mann–Whitney *U*-test. Cut-off levels were determined using receiver operator characteristic curves as the point with the highest area under the curve based on the Youden index. The association of immune parameters with SD status was evaluated using the OR. *P*-values were adjusted for multiple test corrections using the Benjamini–Hochberg adjustment method. We determined the variance inflation factor for the parameters to assess collinearity and then performed multiple logistic regression of parameters with variance inflation factor ≤ 6 . Statistical analysis was performed using MedCalc statistical software (version 14.8.1; MedCalc Software Ltd, Ostend, Belgium; <http://www.medcalc.org>; 2014).

FUNDING SOURCE

Intramural.

CONFLICT OF INTEREST

None of the authors have any conflict of interest to disclose.

AUTHOR CONTRIBUTION

Prashant R Tembhare: Conceptualization; Data curation; Formal analysis; Funding acquisition; Investigation; Methodology; Project administration; Resources; Software; Supervision; Validation; Visualization; Writing-original draft; Writing-review and editing. **Harshini N Sriram:** Data curation; Formal analysis; Investigation; Methodology; Writing-original draft. **Gaurav Chatterjee:** Data curation; Investigation; Methodology; Software; Writing-original draft; Writing-review and editing. **Twinkle Khanka:** Data curation; Investigation; Methodology; Software. **Anant Gokarn:** Data curation; Investigation; Supervision; Writing-original draft. **Sumeet Mirgh:** Data curation; Investigation; Writing-original draft. **Akhil Rajendra:** Data curation; Investigation. **Anumeha Chaturvedi:** Data curation; Formal analysis; Investigation; Methodology; Software. **Sitaram G Ghogale:** Data curation; Formal analysis; Investigation; Methodology. **Nilesh Deshpande:** Investigation; Methodology. **Karishma Girase:** Investigation; Methodology. **Kajal Dalvi:** Data curation; Investigation; Methodology. **Sweta Rajpal:** Investigation; Methodology. **Nikhil Patkar:** Investigation; Methodology. **Bhakti Trivedi:** Data curation; Investigation; Methodology; Supervision. **Amit Joshi:** Data curation; Formal analysis; Investigation; Supervision. **Vedang Murthy:** Data curation; Investigation; Supervision. **Nitin Shetty:** Investigation; Methodology. **Sudhir Nair:** Investigation; Supervision;

Writing-original draft. **Ashwini More:** Investigation; Methodology. **Sujeet Kamtalwar:** Investigation; Methodology. **Preeti Chavan:** Investigation. **Vivek Bhat:** Investigation; Methodology. **Prashant Bhat:** Project administration; Resources; Supervision; Writing-original draft. **Papagudi G Subramanian:** Data curation; Formal analysis; Investigation; Methodology; Validation; Visualization; Writing-original draft; Writing-review and editing. **Sudeep Gupta:** Funding acquisition; Project administration; Resources; Supervision; Writing-original draft; Writing-review and editing. **Navin Khattry:** Conceptualization; Data curation; Funding acquisition; Project administration; Resources; Supervision; Validation; Writing-original draft; Writing-review and editing.

ETHICAL APPROVALS

This study has been approved by the Institutional Ethical Committee. Informed consent was obtained from all individual participants included in the study. Patients signed informed consent regarding publishing their data and photographs.

DATA AVAILABILITY STATEMENT

The data sets generated during and/or analyzed during the current study are available from the corresponding author on reasonable request.

REFERENCES

- Cucinotta D, Vanelli M. WHO declares COVID-19 a pandemic. *Acta Biomed* 2020; **91**: 157–160.
- <https://covid19.who.int/> accessed on May 2, 2021.
- Weiss P, Murdoch DR. Clinical course and mortality risk of severe COVID-19. *Lancet* 2020; **395**: 1014–1015.
- Xu Z, Li S, Tian S, Li H, Kong L. Full spectrum of COVID-19 severity still being depicted. *Lancet* 2020; **395**: 947–948.
- Chen G, Wu DI, Guo W, *et al.* Clinical and immunological features of severe and moderate coronavirus disease 2019. *J Clin Invest* 2020; **130**: 2620–2629.
- Quirch M, Lee J, Rehman S. Hazards of the cytokine storm and cytokine-targeted therapy in patients with COVID-19: Review. *J Med Internet Res* 2020; **22**: e20193.
- Azkur AK, Akdis M, Azkur D, *et al.* Immune response to SARS-CoV-2 and mechanisms of immunopathological changes in COVID-19. *Allergy* 2020; **75**: 1564–1581.
- Qin C, Zhou L, Hu Z, *et al.* Dysregulation of Immune Response in Patients With Coronavirus 2019 (COVID-19) in Wuhan, China. *Clin Infect Dis* 2020; **71**: 762–768.
- Rokni M, Ghasemi V, Tavakoli Z. Immune responses and pathogenesis of SARS-CoV-2 during an outbreak in Iran: comparison with SARS and MERS. *Rev Med Virol* 2020; **30**: e2107.
- Wei J, Zhao J, Han M, Meng F, Zhou J. SARS-CoV-2 infection in immunocompromised patients: humoral versus cell-mediated immunity. *J Immunother Cancer* 2020; **8**: e000862.
- Mathew D, Giles JR, Baxter AE, *et al.* Deep immune profiling of COVID-19 patients reveals distinct immunotypes with therapeutic implications. *Science* 2020; **369**: eabc8511.
- Kuri-Cervantes L, Pampena MB, Meng W, *et al.* Comprehensive mapping of immune perturbations associated with severe COVID-19. *Sci Immunol* 2020; **5**: eabd7114.
- Wang J, Jiang M, Chen X, Montaner LJ. Cytokine storm and leukocyte changes in mild versus severe SARS-CoV-2 infection: review of 3939 COVID-19 patients in China and emerging pathogenesis and therapy concepts. *J Leukoc Biology* 2020; **108**: 17–41.
- Nowill AE, de Campos-Lima PO. Immune response resetting as a novel strategy to overcome SARS-CoV-2-induced cytokine storm. *J Immunol* 2020; **205**: 2566–2575.
- Mann ER, Menon M, Knight SB, *et al.* Longitudinal immune profiling reveals key myeloid signatures associated with COVID-19. *Sci Immunol* 2020; **5**: abd6197.
- WHO Clinical management of COVID-19: interim guidance [May;2020]; <https://www.who.int/publications/item/clinical-management-of-covid-19>. 2020. accessed on August 18, 2020.
- https://www.who.int/blueprint/priority-diseases/key-action/COVID-19_Treatment_Trial_Design_Master_Protocol_synopsis_Final_18022020.pdf. accessed on August 18, 2020.
- Parackova Z, Zentsova I, Bloomfield M, *et al.* Disharmonic inflammatory signatures in covid-19: augmented neutrophils' but impaired monocytes' and dendritic cells' responsiveness. *Cells* 2020; **9**: 2206.
- Xiong Y, Liu Y, Cao L, *et al.* Transcriptomic characteristics of bronchoalveolar lavage fluid and peripheral blood mononuclear cells in COVID-19 patients. *Emerg Microbes Infect* 2020; **9**: 761–770.
- Laing AG, Lorenc A, del Molino del Barrio I, *et al.* A dynamic COVID-19 immune signature includes associations with poor prognosis. *Nat Med* 2020; **26**: 1623–1635.
- Abdul-Jawad S, Baù L, Alaguthurai T, *et al.* Acute immune signatures and their legacies in severe acute respiratory syndrome coronavirus-2 infected cancer patients. *Cancer Cell* 2021; **39**: 257–275.
- Lepone LM, Donahue RN, Grenga I, *et al.* Analyses of 123 peripheral human immune cell subsets: defining differences with age and between healthy donors and cancer patients not detected in analysis of standard immune cell types. *J Circ Biomark* 2016; **5**: 5.
- Cai G, Gao Y, Zeng S, *et al.* Immunological alternation in COVID-19 patients with cancer and its implications on mortality. *Oncoimmunology* 2021; **10**: 1854424.
- Grivas P, Khaki AR, Wise-Draper TM, *et al.* Association of clinical factors and recent anticancer therapy with COVID-19 severity among patients with cancer: a report from the COVID-19 and Cancer Consortium. *Ann Oncol* 2021; **32**: 787–800.
- Thakkar A, Pradhan K, Jindal S, *et al.* Patterns of seroconversion for SARS-CoV-2 IgG in patients with malignant disease and association with anticancer therapy. *Nature Cancer* 2021; **2**: 392–399.

26. Kaplan MH. Th9 cells: differentiation and disease. *Immunol Rev* 2013; **252**: 104–115.
27. Zhou R, To K-W, Wong Y-C, *et al.* Acute SARS-CoV-2 infection impairs dendritic cell and T cell responses. *Immunity* 2020; **53**: 864–877.
28. Sánchez-Cerrillo I, Landete P, Aldave B, *et al.* COVID-19 severity associates with pulmonary redistribution of CD1c⁺ DCs and inflammatory transitional and nonclassical monocytes. *J Clin Invest* 2020; **130**: 6290–6300.
29. Collin M, Bigley V. Human dendritic cell subsets: an update. *Immunology* 2018; **154**: 3–20.
30. Campana P, Parisi V, Leosco D, Bencivenga D, Della Ragione F, Borriello A. Dendritic cells and SARS-CoV-2 infection: still an unclarified connection. *Cells* 2020; **9**: 2046.
31. Draxler DF, Madondo MT, Hanafi G, Plebanski M, Medcalf RL. A flowcytometric analysis to efficiently quantify multiple innate immune cells and T Cell subsets in human blood. *Cytometry A* 2017; **91**: 336–350.
32. Wingender G, Kronenberg M. OMIP-030: Characterization of human T cell subsets via surface markers. *Cytometry A* 2015; **87**: 1067–1069.
33. Brando B, Barnett D, Janossy G, *et al.* Cytofluorometric methods for assessing absolute numbers of cell subsets in blood. European Working Group on Clinical Cell Analysis. *Cytometry* 2000; **42**: 327–346.
34. Cossarizza A, Chang HD, Radbruch A, *et al.* Guidelines for the use of flow cytometry and cell sorting in immunological studies (second edition). *Eur J Immunol* 2019; **49**: 1457–1973.
35. Park LM, Lannigan J, Jaimes MC. OMIP-069: Forty-color full spectrum flow cytometry panel for deep immunophenotyping of major cell subsets in human peripheral blood. *Cytometry A* 2020; **97**: 1044–1051.
36. Liechti T, Roederer M. OMIP-058: 30-parameter flow cytometry panel to characterize iNKT, NK, unconventional and conventional T cells. *Cytometry A* 2019; **95**: 946–951.
37. Mair F, Prlic M. OMIP-44: 28-Color immunophenotyping of the human dendritic cell compartment. *Cytometry A* 2019; **95**: 925–926.
38. Staser KW, Eades W, Choi J, Karpova D, DiPersio JF. OMIP-042: 21-color flow cytometry to comprehensively immunophenotype major lymphocyte and myeloid subsets in human peripheral blood. *Cytometry A* 2018; **93**: 186–189.
39. Rhodes JW, Tong O, Harman AN, Turville SG. Human dendritic cell subsets, ontogeny, and impact on HIV infection. *Front Immunol* 2019; **10**: 1088.
40. Kotsakis A, Harasymczuk M, Schilling B, Georgoulas V, Argiris A, Whiteside TL. Myeloid-derived suppressor cell measurements in fresh and cryopreserved blood samples. *J Immunol Methods* 2012; **381**: 14–22.

SUPPORTING INFORMATION

Additional supporting information may be found online in the Supporting Information section at the end of the article.

© 2021 Australian and New Zealand Society for Immunology, Inc.